Orientation dependence of visual hyperacuity contains a component with hexagonal symmetry

Joy Hirsch

Department of Ophthalmology and Visual Science, Yale University School of Medicine, New Haven, Connecticut 06510

Ron Hylton

Department of Physics, Columbia University, New York, New York 10027

Received January 26, 1983; accepted November 1, 1983

Recently we reported that hyperacuity thresholds for separation-discrimination tasks were not smooth functions of spatial variables but rather were regularly segmented with sharp transitions between the segments.[1] In this study we have measured the orientation dependence of two tasks involving visual hyperacuity, the discrimination of spatial frequencies and the discrimination of vernier offsets, in the vicinity of a transition between segments. The orientation dependence of both tasks contains a periodic component with a period of 60°. We interpret this as evidence that the cortical substrate that processes spatial information has a hexagonal two-dimensional organization, preserving the hexagonal packing of the foveal photoreceptors.

INTRODUCTION

Recently we reported that discriminating between spatial frequencies of suprathreshold sinusoidal gratings near and above 4 cycles per degree (c/deg) is a task involving spatial hyperacuity, angular resolutions finer than the center-to-center spacing of foveal photoreceptors.[1] Further, the magnitudes of the hyperacuity thresholds were related to the center-to-center spacing of photoreceptors. We suggested that this relationship was due to a cortical representation of the image that directly reflected the organization of the retinal photoreceptor lattice. A logical consequence of this argument is that the two-dimensional properties of the cortical mechanisms that process spatial information should also reflect the two-dimensional organization of the photoreceptor lattice. In this paper we report evidence that this is indeed the case and that the orientation dependence of two different tasks involving hyperacuity contains a component with hexagonal symmetry (period = 60°), presumably reflecting the hexagonal packing of photoreceptors.[2] In addition, we find that the orientation dependence of vernier-offset discrimination contains another component with square symmetry (period = 90°) and that the phases of the components of the two tasks are not arbitrary. We present a specific model for the origin of the hexagonal component.

METHODS

Two different tasks were employed: discriminating between spatial frequencies of suprathreshold sinusoidal gratings and discriminating the direction of the vernier offset of two narrow lines. In both experiments stimuli were electronically generated on an oscilloscope screen (Tektronix 606). A single experimental session measured a threshold for a particular orientation, so that the orientation of all patterns remained constant during each session. Different orientations were set for different sessions by physically rotating the display, which was a 4-deg circular field set in a 12-deg circular surround matched in hue and brightness to the central display field. The orientation for each session was chosen in an irregular order separately for each observer and task. Observers in both experiments were seated 150 cm from the stimulus screen. Head stabilization was achieved by a chin-and-forehead rest modified to include bilateral head supports.

In the case of the spatial-frequency-discrimination experiments, sinusoidal gratings were displayed at 30% contrast. Each session employed a constant reference frequency and a set of nine test frequencies chosen symmetrically around the reference. Each trial consisted of a 0.75-sec presentation of the reference grating, a 0.75-sec interstimulus interval, and a 0.75-sec presentation of one of the test gratings. Spatial phase was randomized on each presentation for both reference and test gratings independently. The order of test presentations was randomized according to the method of constant stimuli, and each test pattern was presented 50 times. Following each trial the observer indicated whether the test frequency was higher or lower than the reference and was given feedback by a synthesized voice indicating the true relationship. The probability distributions were fitted to a cumulative normal distribution, and the just noticeable difference (jnd) in frequency (Δf) was defined as the change in frequency necessary to increase the probability of a correct response from 0.5 to 0.75. The fitting procedure also estimated the statistical error in Δf. Full details of the spatial-frequency-discrimination experiments were reported previously.[1]

The vernier-offset experiments were identical in all respects with the spatial-frequency-discrimination experiments, except that each presentation of a grating was replaced by the presentation of a vernier-discrimination target consisting of two narrow line segments, each 0.25 deg long, separated by a gap of 0.25 deg. For the reference pattern the two lines were collinear; the test patterns had small perpendicular offsets. The overall position of the target was randomly offset from

07403232/84/030300-09$02.00

the center of the screen for the test and reference patterns independently on each trial by up to 0.2 deg. The task of the observer was to determine the direction of the vernier offset, and the jnd in offset (Δo) was determined as for Δf. Orientation for different sessions was again varied by physically rotating the screen.

Two well-practiced observers participated in this experiment. Neither wore any optical correction during the experiment. Visual acuity for JH was 20/20 in each eye with no astigmatism, and the axial length for her right eye was 22.2 mm. Visual acuity for SC was also 20/20 in each eye with no astigmatism. The axial length for her right eye was 22.1 mm. Neither observer had any history of eye disease, and we assume that both observers are representative of normal vision.

RESULTS

The results of the spatial-frequency experiments are shown in Fig. 1 for observer SC at a reference frequency of 4.0 c/deg and for observer JH at a reference frequency of 4.5 c/deg. As is discussed below, these reference frequencies were chosen in the expectation (derived from our model of spatial-frequency discrimination) that they would maximize the hexagonal orientation effects predicted above. The figure shows the fractional jnd in spatial frequency $\Delta f/f$ (f is the reference frequency) plotted against the orientation of the grating, where an orientation of 0° corresponds to the usual vertical grating. The data are clearly not constant but show significant variation with orientation.[3] Multiple data points are repeated measurements over time and show good stability.[4] The curves are fits to the data and are discussed in detail below.

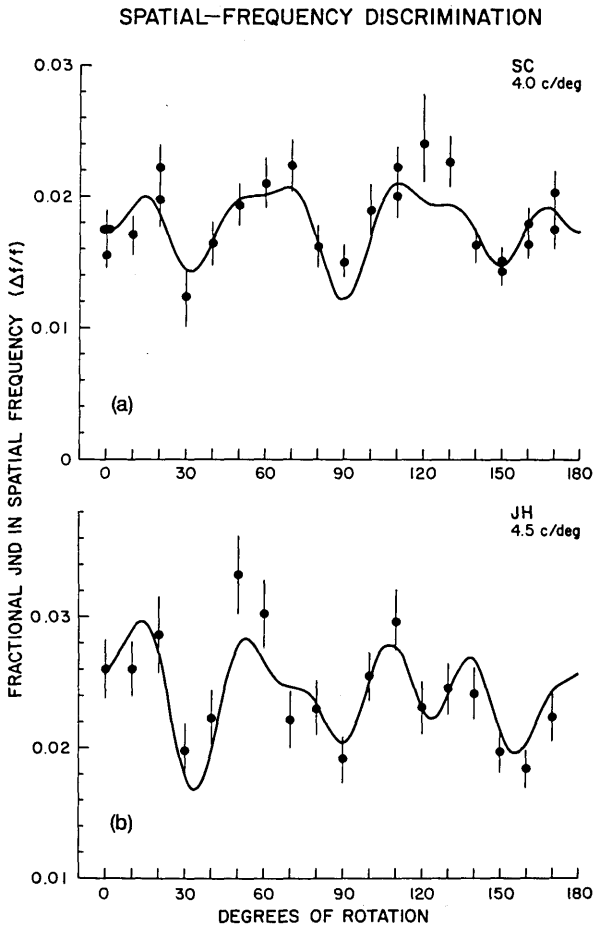

Fig. 1. Fractional jnd in spatial frequency, $\Delta f/f$, where Δf is the jnd in frequency and f is the reference frequency, as a function of orientation. 0° represents the vertical (bar) grating orientation. Functions are shown (a) for observer SC for a reference frequency of 4.0 c/deg and (b) for observer JH for a reference frequency of 4.5 c/deg.

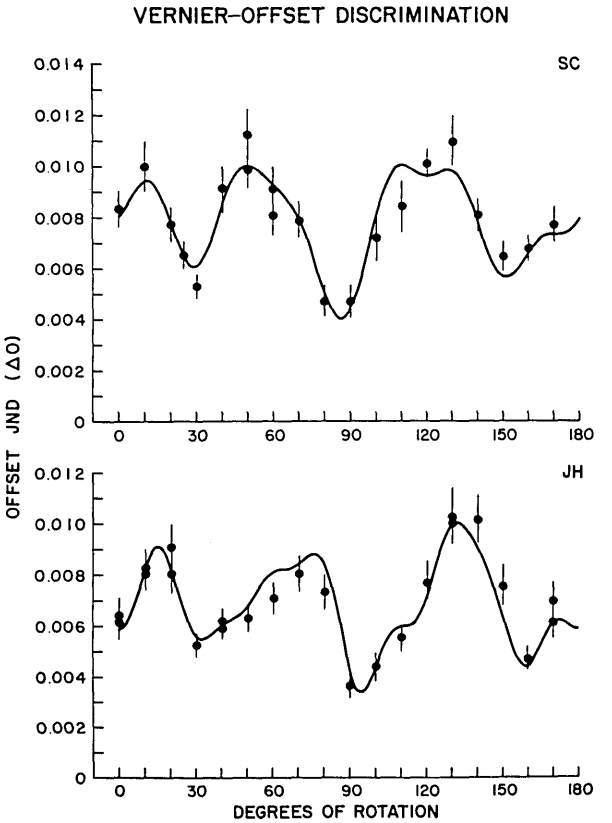

Fig. 2. Jnd in offset, Δo, for the vernier-offset-discrimination task as a function of orientation, where 0° represents the horizontal orientation of line segments. Functions are shown for two observers SC and JH with a gap of 0.25 deg in the vernier target.

Figure 2 shows the results for the vernier-discrimination experiments for the same two observers with the gap in the vernier target equal to 0.25 deg, also chosen in the expectation of a maximal hexagonal effect. The vernier-offset thresholds are plotted against the orientation of the stimulus, where an orientation of 90° corresponds to the usual vertical vernier target. This choice is not arbitrary but is required to align the vernier-discrimination data with the spatial-frequency-discrimination data. The vernier thresholds also clearly depend on orientation and are stable over time, as indicated by multiple determinations.

DATA ANALYSIS

We find that the orientation dependence of the data presented above consists of the sum of two periodic components, one with hexagonal symmetry (60° period) and the harmonics thereof and the other with square symmetry (90° period) and its harmonics. The most general form for a component with period L is

$$f(x) = \sum_{N=1}^{M} a_N \cos(2\pi Nx/L) + b_N \sin(2\pi Nx/L). \quad (1)$$

However, we also require that there be no difference between positive and negative rotation, leading to the more restricted form

$$f(x) = \sum_{N=1}^{M} a_N \cos[2\pi N(x - x_0)/L], \quad (2)$$

which has even symmetry around some unknown symmetry axis x_0. The value of M (the number of harmonics) is in principle determined by sampling requirements, but in practice $M = 2$ suffices for all the data reported here except for the JH vernier-discrimination data, which require some higher harmonics of the square component to achieve a good fit.[5,6]

Table 1 shows the results of fitting the data in Figs. 1 and 2 to four different models of orientation dependence: (1) no orientation dependence, (2) the orientation dependence consists of a hexagonal component only, (3) a square component only, and (4) the sum of a square and hexagonal component. The chi-squared (χ^2) values, the degrees of freedom, and levels of confidence for the fits are listed in the table. A large chi-square indicates that the deviations of the data from the model are larger than can be accounted for by the error bars. Both frequency-discrimination observers have marginally acceptable fits for the hexagonal-only model and good fits for the hexagonal-plus-square model, while the square-only model is rejected. The hexagonal-plus-square model gives a good fit for both vernier-discrimination observers, while all other models are rejected. The fits to the hexagonal-plus-square model are shown in Figs. 1 and 2 (dark lines through the data).

The hexagonal and square components are evaluated separately in Table 2, where we test the significance of the difference in chi squared between the hexagonal-plus-square model and either the hexagonal-only or the square-only model. If the omitted component is not significant, the difference in chi-square should be attributable to the difference in the number of degrees of freedom between the models being compared. Thus a large chi-square here indicates that we can reject the null hypothesis that the amount of variance attributed to the component under consideration is statistically insignificant. The hexagonal component is extremely significant ($p < 0.001$) for all four sets of data. The square components are quite significant for the two sets of vernier-discrimination data ($p < 0.001$) but of modest significance (p is a few percent) for both sets of frequency-discrimination data.

The decomposition of the total orientation dependence into hexagonal and square components is shown in Fig. 3. The middle plot in each of the four parts shows the fit to the hexagonal-plus-square model along with the data from Figs. 1 and 2 with the mean value subtracted. Immediately above and below each fit is separately plotted the hexagonal and the

Table 1. Fits to Models of Orientation Dependence

Type of Discrimination	Observer	Orientation Dependence	χ^2	Degrees of Freedom	Level of Confidence
Spatial frequency	SC	none	69.5	24	3×10^{-6}
	(4.0 c/deg)	hexagonal	33.9	21	0.037
		square	67.0	21	1×10^{-6}
		hex. plus square	26.5	18	0.088
	JH	none	40.7	17	0.001
	(4.5 c/deg)	hexagonal	22.7	14	0.065
		square	33.0	14	0.003
		hex. plus square	13.4	11	0.270
Vernier offset	SC	none	139.0	20	$<10^{-10}$
(gap, 0.25 deg)		hexagonal	57.5	17	3×10^{-6}
		square	96.3	17	$<10^{-10}$
		hex. plus square	17.9	14	0.210
	JH	none	161.3	23	$<10^{-10}$
		hexagonal	66.6	20	7×10^{-7}
		square	125.1	18	$<10^{-10}$
		hex. plus square	18.4	15	0.240

Table 2. Significance of Orientation Components

Type of Discrimination	Observer	Component	χ^2	Degrees of Freedom	Level of Confidence
Spatial Frequency	SC	hexagonal	40.5	3	8×10^{-9}
	(4.0 c/deg)	square	7.4	3	0.060
	JH	hexagonal	19.7	3	2×10^{-4}
	(4.5 c/deg)	square	9.3	3	0.025
Vernier Offset	SC	hexagonal	78.4	3	$<10^{-10}$
(gap, 0.25 deg)		square	39.6	3	1×10^{-8}
	JH	hexagonal	106.7	3	$<10^{-10}$
		square	48.2	5	3×10^{-9}

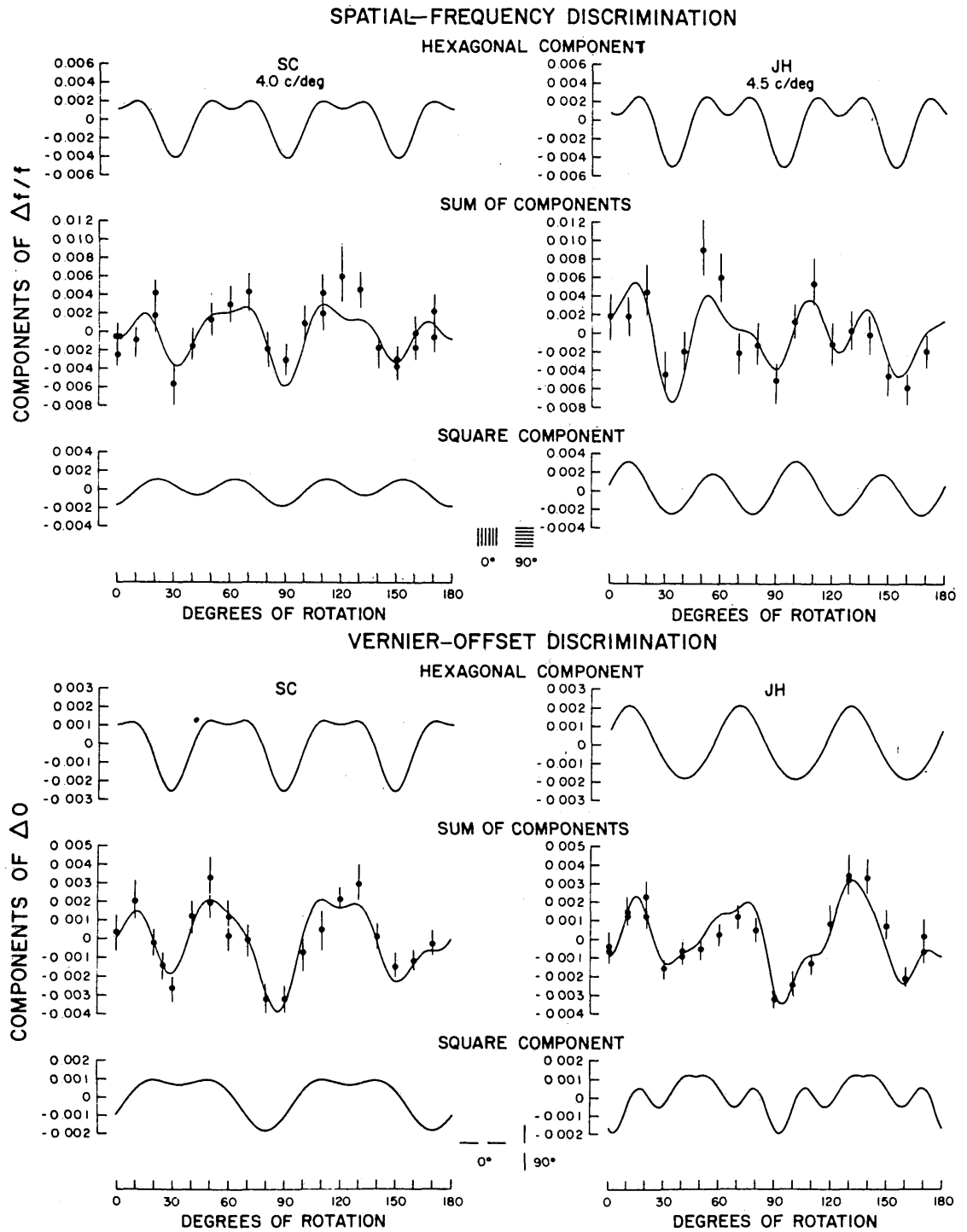

Fig. 3. The decomposition of orientation dependence into hexagonal and square components for the spatial-frequency-discrimination task (upper sections) and for the vernier-offset-discrimination task (lower sections). Center plot in each quadrant shows the sum of hexagonal and square components plus the data replotted from Figs. 1 and 2 (minus the average). Note that 0° rotation is a vertical spatial-frequency grating (top graphs) and a horizontal vernier line segment (bottom graphs).

square components, respectively. There are a number of noteworthy features. First, the phases of the hexagonal components are fairly closely aligned across tasks and across observers, having a minimum near 90°. Whereas this orientation represents a vertical vernier target, the corresponding grating is horizontal. This is an important observation since it demonstrates that the orientation on which the hexagonal component primarily depends is not the orientation along which the jnd is being measured (the jnd's are measured along orthogonal directions for vertical vernier targets and horizontal gratings) but some other direction, and a possible explanation is given below. The square component for the vernier data also has a minimum near 90° (and 0°). The square components for the spatial-frequency data (which are only marginally statistically significant) seem to be more octagonal (period = 45°) than square.

The results above show that a model consisting of the sum of a hexagonal plus a square component, each with even symmetry, is sufficient to explain the observed orientation functions reported here, and both components are necessary within this model. As is discussed in Appendix A, the necessity of including both the hexagonal and the square components can also be established in a strong model-independent manner, leading to the conclusion that it is essentially impossible for any model that lacks either component to fit the data.

DISCUSSION

These results demonstrate that the hyperacuity thresholds reported here display an orientation anisotropy having components with both hexagonal and square symmetry. This effect cannot be an artifact since our display apparatus was circularly symmetric. Although a square component, or oblique effect, is most often reported in spatial tasks as a function of orientation,[7–10] Caelli *et al.* have recently reported spatial-frequency-discrimination data that also clearly show a strong 60° periodicity for one observer and what appears to be a mixture of 60° and 90° components for other observers.[11] Since, in our study, two quite different tasks, spatial-frequency discrimination and vernier-offset discrimination, both show a hexagonal component, we conclude that the underlying cause must be general. Extending arguments made previously, we attribute the hexagonal orientation anisotropy of hyperacuity to the existence of a cortical representation of an image, which we refer to as a neural lattice, that preserves the hexagonal symmetry of the retinal photoreceptor lattice. We present below a specific model to explain the manifestation of the hexagonal symmetry in tasks involving the measurement of spatial separations. This model does not account for all orientation effects in spatial vision, and in particular the origin of the square component is not addressed.

The Hexagonal Component

The basic proposal that we make for the hexagonal component is quite simple: The human visual system does not measure separations or distances in arbitrary directions. Rather there exists a set of intrinsic directions fixed by the orientation of the observer's head and the hexagonal structure of the photoreceptor lattice, and distance is assumed to be measured parallel to one of these directions. As a consequence, the effective distance between two parallel lines is not necessarily the perpendicular distance but rather the distance measured along one of the intrinsic directions, presumably the one closest to the perpendicular. The usual identification of the perpendicular distance as the true, or objective, distance rests on the unstated assumption that the visual system possesses rulers at every possible orientation. However, the hexagonal symmetry reported here suggests that there are only three such intrinsic measurement directions, separated by 60°, presumably attributable to cortical reflection of the hexagonal photoreceptor packing.

More specifically, we have previously argued that the human visual system measures distances (and spatial frequencies) by identifying features on a neural lattice (for instance, two successive peaks in the case of a sine-wave grating or perhaps points of inflection,[12] the exact feature being irrelevant here) and then counting the number of lattice points separating them. We make here the additional suggestion that this counting can be done only along the basis directions of the lattice, the directions for which the lattice is most closely spaced. The net result is an enormous reduction in the complexity of the distance-measuring mechanism since it need not deal with arbitrary directions, but at the price of potentially introducing orientation-dependent errors in distance measurements. If the perpendicular distance between two lines is s_p, the effective distance measured along one of the intrinsic lattice directions is $s_p/\cos(A)$, where A is the angle between the perpendicular and the nearest lattice direction. Since the intrinsic lattice directions are separated by 60°, A cannot exceed 30°, and the maximum effect is an effective distance $s_e = s_p/\cos(30°) = 1.15s_p$, or a ±7.5% maximum. The typical error introduced by this mechanism is given by the standard deviation of $\cos(A)$ between ±30°, which is 4%. The smallness of the effect is due to the flatness of the cosine function over a considerable region around zero. Since spatial frequencies are proportional to $1/s$, the effective spatial frequency f_e will be $f_e = f_p \cos(A)$, where f_p is the frequency measured perpendicular to the wave fronts. Note that effective distances are always larger and the effective spatial frequencies are always lower than the corresponding perpendicular measurements. [The above arguments assume perpendicular projections onto the lattice directions. The projections might instead involve some sort of dogleg along the lattice directions, modifying the above formulas somewhat. The magnitude of the effect is unchanged, and effective distances are again always larger, but the exact relationship becomes

$$s_e = s_p * \cos(30° - A)/\cos(30°).]$$

Since the expected hexagonal orientation effects derived above are fairly small, it follows that they would be difficult to observe directly. However, we have previously shown that at certain transition frequencies spatial-frequency discrimination is a rapidly changing function of frequency, and this can be used to amplify the effect. Figure 4 shows $\Delta f_p/f_p$ as a function of the reference frequency f_p for gratings at 0° or-

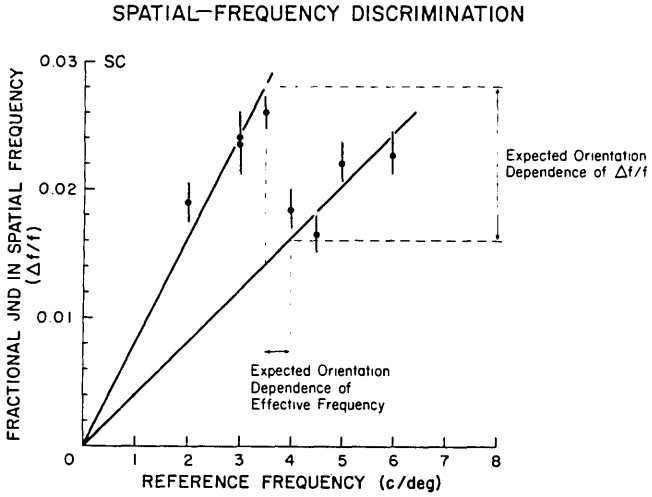

Fig. 4. Fractional jnd in spatial frequency, $\Delta f/f$, as a function of reference frequency for observer SC. The data show a sharp transition between 3.5 and 4 c/deg. This effect has been previously described.[1] The dashed lines illustrate the use of the transition to magnify an anticipated small hexagonal orientation effect, as discussed in the text.

ientation (vertical) for observer SC. We have previously shown that this function consists of segments that are straight lines passing through the origin (drawn in the figure) separated by transition regions (the first at ~4 c/deg) where $\Delta f_p/f_p$ falls rapidly with frequency.[1] Given the arguments above, we should have plotted $\Delta f_e/f_e$ as a function of f_e, where f_e is the effective frequency as measured by the observer. Since $\Delta f_e/f_e = \Delta f_p/f_p$, the y axis is unchanged, but all values on the x axis should actually be replaced by $f_p \cos(A - A_0)$, where A is 0° for all points on the graph and A_0 is the closest intrinsic measurement direction. For simplicity assume that A_0 is 0° and the x axis is actually f_e. Suppose that we tested observer SC at a nominal frequency of 4.0 c/deg and an orientation of 0°. Then we should get the value of $\Delta f/f$ shown in Fig. 4 (~0.016). Now suppose that we changed the grating orientation by 30° while keeping the perpendicular frequency fixed. This reduces the effective frequency to $4.0 * \cos(30°) = 3.5$ c/deg, and we should now measure $\Delta f/f \sim 0.028$. In effect changing the orientation by 30° causes the effective frequency to walk along the x axis in Fig. 4 from 4.0 to 3.5 c/deg, and $\Delta f/f$ should vary by the corresponding amount on the y axis. Increasing A to 60° causes f_e to walk back to 4.0 c/deg. Inspecting Fig. 1(a) and allowing for the fact that A_0 was not actually 0° indicates that this is nearly the case, with the orientation data oscillating roughly between the limits expected from Fig. 4. The orientation data were somewhat lower than expected, perhaps partially because of some contribution from the square component or a small practice effect. Note also that the nonlinearity in the frequency-discrimination function near the transition will lead to a potentially complicated shape for the hexagonal component even though the effective frequency is a fairly simple function of orientation.[13] Actually the fitted hexagonal components (Fig. 3) have relatively narrow dips and fairly flat maxima, possibly indicating that the effective frequency walked to the top of the transition in Fig. 4 and then started moving down the first segment. The results for JH are similar, with the transition occurring at a somewhat higher frequency.[1] Notice that we have exploited the transition region in Fig. 4, where $\Delta f/f$ is a rapidly changing function of f, in order to magnify the expected small effects of orientation and produce the striking results of Fig. 1.[14] At higher frequencies the transitions are smaller, and we expect the hexagonal component to be smaller. The exact shape of the hexagonal component for the two tasks is almost identical for observer SC but not for JH. However, we do not believe that there is any reason to expect that the shape should be exactly the same for the two tasks since we expect that it depends quite critically on aligning the transitions for the two tasks (shown in Fig. 4 for frequency discrimination and discussed below for vernier discrimination). Indeed, we expect the shape of the component to vary quite strongly for both tasks as the spatial frequency or gap size is varied because of the severe nonlinearity of the frequency-discrimination function near the transition regions.

Arguments identical with the ones above can be used to explain the hexagonal component in the variation of vernier discrimination as a function of line-segment orientation. Vernier-offset thresholds have been shown to be a function of the length of the gap between the two lines.[15] The effective length of a gap will vary with orientation similarly to the effective period of a grating, and if the vernier-threshold versus gap-size function shows transitions comparable with those in spatial-frequency discrimination the expected small hexagonal component will be magnified.[16] Further, this explains why the hexagonal component has a minimum for vertical vernier targets and horizontal spatial-frequency gratings. As can be seen in Fig. 3, the hexagonal components of the two tasks are in phase when the gap of the vernier stimulus is perpendicular to the bars of the grating and thus aligned with the direction between bars along which spatial frequency is measured. This is consistent with our expectation that the variable that primarily determines the hyperacuity threshold (the scale-setting variable) is the gap for a vernier target and the distance between bars for a grating. Note also that the two observers are nearly in phase with respect to the hexagonal component. If, as we propose, the hexagonal component is fundamentally attributable to the photoreceptor lattice, this suggests that the photoreceptor lattice has a fixed orientation and likely has the same orientation in both eyes.

The data presented here measure the ability of observers to discriminate differences in position or spatial frequency as a function of orientation. However, if we identify the effective spatial variables described above with the perceptual variables of spatial distance and frequency, then the model that we have presented to account for the hexagonal component of the variation of jnd's with orientation may very well imply the existence of systematic hexagonally symmetric orientation-dependent biases in the perception of spatial distances and frequencies. The existence of such effects, however, does not unavoidably follow from the model since systematic errors are always in principle correctible and therefore may be automatically removed from perception. Variations in apparent spatial frequency with stimulus orientation have recently been reported.[17–19] However, since only four or fewer orientations were sampled in those studies, it is not possible to determine if a hexagonal component was present, and indeed aliasing of undersampled hexagonal components is a potential problem for those measurements. However, we estimate above that such effects will be small and perhaps difficult to detect in the absence of a mechanism to amplify them.

One further significant point is that the existence of such well-defined orientation effects demonstrates that some part of the visual system, presumably the photoreceptor lattice, possesses a well-defined geometry over regions at least as large as the stimuli employed in this experiment (several tenths of a degree) and probably larger, since we made no attempt to stabilize the image on the retina but rather randomized its position by several tenths of a degree on each trial. This is inconsistent with a recent report by Yellott suggesting that the primate photoreceptor lattice is highly disordered.[20] However, analysis of electron micrographs of primate-cone inner segments published by Miller[2] shows clearly that the foveal lattice is a high-quality hexagonal lattice at least over spans of tens of photoreceptors, and this is probably adequate to provide the physiological basis for the results reported here.[21]

The Square Component

The square component observed in the vernier-discrimination data is presumably related to the commonly reported oblique effect. Although the origin of the square component is not discussed in this paper, we assume that the mechanism

underlying the square component is distinct from the mechanism underlying the hexagonal component, with which we are primarily concerned here. It should be noted that the square component shows far less task-to-task consistency in our data than does the hexagonal component, possibly indicating a less fundamental origin.

CONCLUSION

Guided by an extension of our previously reported model of spatial-frequency discrimination, we have shown that hyperacuity thresholds as a function of stimulus orientation contain a component with hexagonal symmetry. We assume that this hexagonal symmetry is fundamentally related to the hexagonal packing of photoreceptors. Since the magnitudes of similar hyperacuity thresholds have previously been related to the center-to-center spacing of photoreceptors,[1] we conclude that there is now strong evidence for the role of the photoreceptor lattice in spatial vision. In addition, at least some spatial tasks have a component with square symmetry in their orientation dependence. We propose a model of spatial vision in which the photoreceptor lattice provides the only geometrical element, with all other elements being topological.

APPENDIX A: MODEL-FREE ANALYSIS OF ORIENTATION DEPENDENCE

In this appendix we present an analysis of the orientation dependence of the data reported above that is independent of any model. The analysis starts from the observation that, if our data consisted of exactly one measurement every 10° of rotation, they could be exactly fitted by a Fourier series of the form

$$F(x) = a_0 + \sum_{N=1}^{8} [a_N \cos(2\pi Nx/180) + b_N \sin(2\pi Nx/180)] + a_9 \cos(2\pi 9x/180)$$

(the sin term for harmonic 9 vanishes identically). However, for all but the JH frequency-discrimination data, there are multiply determined points or points not on 10° intervals. For these the above series gives a fit that is not exact but is in practice so close to being perfect that we can consider it to be exact. Hence this series is the most general possible model for the orientation dependence of our data. Then the function given by the series above, but with a particular harmonic (value of N) omitted, is the most general possible model that lacks this harmonic. By fitting our data with such a function we can test whether any model that lacks a particular harmonic is capable of fitting the data. This is an extremely strong test for the necessity of a given harmonic, since if the chi-square for a fit to this function is even moderately large it will be nearly impossible to construct a model that lacks this harmonic and still fits the data. We can also construct a somewhat weaker but still interesting test by considering the change in chi-square caused by omitting a given harmonic from the series above rather than the overall goodness of fit chi-square. If the change in chi-square is larger than can be attributed to the change in the number of degrees of freedom, then this indicates that the omitted harmonic is present at a statistically significant level. This does not establish the necessity of the harmonic, since by judicious choice of which terms are included or excluded it may still be possible to construct a model that lacks the harmonic but still gives an acceptable overall fit. However, if the change in chi-square is sufficiently large, such a manipulation of the overall chi-square and degrees of freedom will be quite difficult. Note that, because of the unequal spacing and unequal error bars, the sines and cosines above do not form an orthogonal set. There are modest correlations between them (typically 0.1), and changes in chi squared caused by omitting two harmonics will not be exactly equal to the sum of the chi-squared changes for omitting each separately.

The results of applying the above procedure to our data are given in Tables 3 and 4. The column χ^2_{fit} gives the overall goodness of fit chi-square for the function given by the series above with the noted harmonics omitted. The column χ^2_{sig} gives the change in chi-square caused by the omission of the harmonics. The asterisks after confidence levels indicate those chi-squares with a confidence level of less than 0.01.

It is clear that in all four sets of data we can reject any model that lacks harmonic 3, the fundamental of the hexagonal component (period = 60°). For the two sets of vernier-discrimination data we can also reject any model that lacks harmonic 2, the fundamental of the square (or oblique) component (period = 90°). The two sets of frequency-discrimination data show no evidence for the square component but show some evidence for harmonic 4 (period = 45°). This

Table 3. Harmonic Analysis of Spatial-Frequency Discrimination[a]

	Subject											
	SC (4.0 c/deg)						JH (4.5 c/deg)					
Omitted Harmonics	χ^2_{fit}	Degrees of Freedom	Level of Confidence	χ^2_{sig}	Degrees of Freedom	Level of Confidence	χ^2_{fit}	Degrees of Freedom	Level of Confidence	χ^2_{sig}	Degrees of Freedom	Level of Confidence
none	4.4	7	0.73	–	–	–	0	0	–	–	–	
1	13.8	9	0.13	9.3	2	0.009*	4.9	2	0.086	4.9	2	0.086
2	7.5	9	0.58	3.1	2	0.21	3.6	2	0.16	3.6	2	0.16
3	34.6	9	7×10^{-5}*	30.2	2	3×10^{-7}*	14.4	2	7×10^{-4}*	14.4	2	7×10^{-4}*
4	9.4	9	0.40	5.0	2	0.082	11.1	2	0.004*	11.1	2	0.004*
5	9.6	9	0.38	5.2	2	0.073	0.5	2	0.79	0.5	2	0.79
6	7.8	9	0.56	3.4	2	0.18	7.9	2	0.19	7.9	2	0.019
7	9.8	9	0.37	5.4	2	0.067	2.0	2	0.36	2.0	2	0.36
8	6.1	9	0.73	1.6	2	0.44	0.3	2	0.87	0.3	2	0.87
9	4.8	8	0.78	0.3	1	0.56	0.2	1	0.68	0.2	1	0.68

[a] Asterisks indicate chi-squares with confidence level of less than 0.01.

Table 4. Harmonic Analysis of Vernier-Offset Discrimination[a]

	Subject											
	SC						JH					
Omitted Harmonics	χ^2_{fit}	Degrees of Freedom	Level of Confidence	χ^2_{sig}	Degrees of Freedom	Level of Confidence	χ^2_{fit}	Degrees of Freedom	Level of Confidence	χ^2_{sig}	Degrees of Freedom	Level of Confidence
none	2.3	3	0.51	–	–	–	2.2	6	0.91	–	–	–
1	6.6	5	0.26	4.2	2	0.12	14.2	8	0.076	12.1	2	0.002*
2	29.6	5	2×10^{-5}*	27.2	2	1×10^{-6}*	27.8	8	5×10^{-4}*	25.7	2	3×10^{-6}*
3	56.7	5	6×10^{-11}*	54.4	2	2×10^{-12}*	95.7	8	$<10^{-12}$	93.5	2	$<10^{-12}$
4	7.5	5	0.19	5.1	2	0.076	2.6	8	0.95	0.5	2	0.78
5	4.6	5	0.47	2.3	2	0.32	2.7	8	0.95	0.5	2	0.77
6	10.3	5	0.068	8.0	2	0.019	12.1	8	0.15	9.9	2	0.007*
7	4.7	5	0.46	2.3	2	0.31	5.2	8	0.73	3.1	2	0.21
8	2.4	5	0.79	0.1	2	0.96	5.3	8	0.73	3.1	2	0.21
9	2.5	4	0.65	0.1	1	0.72	2.5	7	0.93	0.3	1	0.59

[a] Asterisks indicate chi-squares with confidence level of less than 0.01.

would be the second harmonic of the square (oblique) component and confirms the observation above that the frequency-discrimination data contain more an octagonal than a square component. Interestingly, two of the sets of data show some evidence for the $N = 1$ harmonic (period = 180°). Although this component does not have the extreme statistical significance of the others noted above, its presence would have the effect of spoiling the square symmetry so that horizontal and vertical could never be exactly identical, even in the absence of the hexagonal component.

ACKNOWLEDGMENTS

We thank our observer, Steffanie E. Crowley, and Jan McVey, postdoctoral fellow, for refractions and axial-length measurements. Portions of this paper were presented at the annual meeting of the Association for Research in Vision and Ophthalmology in 1983. This work was partially supported by grants EY 00785 and EY00167 from the National Eye Institute, Research to Prevent Blindness, the Connecticut Lions Eye Research Foundation Association, and grant 49620-83-C-0026 from the U.S. Air Force Office of Scientific Research, Air Force Systems Command.

REFERENCES

1. J. Hirsch and R. Hylton, "Limits of spatial frequency discrimination as evidence of neural interpolation," J. Opt. Soc. Am. **72,** 1367–1374 (1982).
2. W. H. Miller, "Intraocular filters," in *Handbook of Sensory Physiology* (Springer-Verlag, New York, 1979), Vol. VII/5, pp. 70–135.
3. D. O. Bowker ["Spatial frequency discrimination thresholds in different orientations," J. Opt. Soc. Am. **70,** 462–463 (1980)] studied the orientation dependence of spatial-frequency discrimination at several reference frequencies including 4 c/deg. He reported no evidence for orientation dependence at this frequency. There are two possible explanations for the discrepancy between those observations and the observations reported here. First, we find that the choice of reference frequency is fairly critical, as is discussed in more detail below. Second, in the Bowker study, the orientation function was sampled only at 45° intervals, which is below the sampling limit for all harmonics of the hexagonal component and also for all but the fundamental of the square component. Indeed, aliasing of these higher-frequency components is a potentially serious problem with such a coarse sampling.
4. S. P. McKee and G. Westheimer ["Practice effects of orientation," Percept. Psychophys. **24,** 258–262 (1978)] have reported that the effects of orientation on vernier acuity decreased substantially after practice. To avoid practice effects observer SC completed more than 8000 trials of preliminary data before the final data reported here were collected, and JH, an extremely experienced observer, completed at least 4000 initial trials. Although the effects of large numbers of repetitions were not studied here, the essential results were replicable over the three-month period of data collection. A possible explanation for the practice effect may be subtle head movements employed by the observer to improve performance on nonpreferred stimulus orientations. We encountered such a problem and solved it by improving head stabilization. This is an interesting point in that it indicates that observers may be to some degree aware of the existence of optimal orientations and attempt to tilt their heads to exploit them.
5. The models that we consider have one parameter for the mean value of the function plus one phase (x_0) and M amplitudes for each of the two components (hexagonal and square, $L = 60°$ and $L = 90°$, respectively). The value of M is the number of harmonics of the fundamental periodic component used in the fit. These harmonics are locked in phase with the fundamental and represent the shape of the component, which is not expected to be a simple sinusoid (see the discussion of Fig. 4). For all but the JH vernier-discrimination data M equals 2 for both components, for a total of seven parameters. For the JH vernier data the square component has $M = 4$, for a total of nine parameters. Adding more components does not give a statistically significant improvement in any of the fits. Note that the third harmonic of the square component and the second harmonic of the hexagonal component both have a period of 30° and will be difficult to distinguish if their phases are too close. The choice of sine waves as the basis functions is essentially arbitrary and occurs because we do not know exactly what the shape of the two components should be.
6. The orientation data are fitted by adjusting the parameters of the model to minimize chi-square, defined as the sum over observations of Z^2_{obs}, where Z_{obs} is the difference between the model prediction and the observed value divided by the estimated error in the observation. This is not a theoretically exact chi-squared statistic because of the use of errors estimated from the psychophysical fitting procedure rather than the true errors (which are unknown). In the univariate case this theoretically calls for a t test instead of a Z test. However, because of the large number of trials per session (450) the error in the estimated errors is small, a point that is confirmed by the repeated measurements in this experiment and in previous experiments using similar techniques. Hence we treat this chi-square as a true chi-squared statistic, which is equivalent to the common use of a Z test instead of a t test when the number of trials is large. We have also repeated all our analyses using F tests comparing the variance explained by the model with the residual variance and have come to identical statistical conclusions, although the F tests are also not quite theoretically exact since different points have different errors.

7. D. E. Mitchell, R. D. Freeman, and G. Westheimer, "Effect of orientation on the modulation sensitivity for interference fringes on the retina," J. Opt. Soc. Am. **57,** 246–259 (1967).
8. E. Matin and A. Drivas, "Acuity for orientation measured with a sequential recognition task and signal detection methods," Percept. Psychophys. **25,** 161–168 (1979).
9. C. W. Tyler, "Orientation differences for perception of sinusoidal line stimuli," Vision Res. **17,** 83–88 (1977).
10. S. Appelle, "Perception and discrimination as a function of stimulus orientation: the 'oblique effect' in man and animals," Psychol. Bull. **78,** 266–278 (1972).
11. T. Caelli, H. Brettel, I. Rentschler, and R. Hilz, "Discrimination thresholds in the two-dimensional spatial frequency domain," Vision Res. **23,** 129–133 (1983). The most detailed data of Caelli *et al.* are presented in a two-dimensional form that is difficult to compare with the data presented here. However, they display summary graphs showing spatial-frequency discrimination as a function of orientation averaged over 4, 8, and 12 c/deg, which are coincidentally the nominal frequencies at which we expect transitions to occur. For one of their observers (RH, Fig. 2d) this function displays an almost pure 60° periodicity although it lacks the even symmetry that we expect, perhaps because of averaging over several transitions. The data for the other two observers (TMC and IR, Figs. 1d and 2d) are less clear but appear to be a mixture of hexagonal and square components, as is reported here.
12. R. J. Watt and M. J. Morgan, "Mechanisms responsible for the assessment of visual location: theory and evidence," Vision Res. **23,** 97–109 (1983).
13. The complete theoretical hexagonal dependence consists of three parts: First there is the angular deviation between the orientation being tested and the nearest intrinsic direction. This is given by

$$A_H(A) = [(A - A_0 + 30°)\text{modulo } 60°] - 30°,$$

where A is the orientation and A_0 is one of the intrinsic directions. Thus $A_H(A)$ is a sawtooth wave of period 60°, which ranges linearly from −30° to +30° and then abruptly back to −30° as A is varied through 60°, with $A_H = 0$ when A corresponds to one of the intrinsic directions. This angular error (A_H) leads to an orientation-dependent effective frequency given by $f_e(A) = f_p \cos[A_H(A)]$, where f_p is the perpendicular or nominal frequency, although one variant of our model would use 1/cos instead of cos. Since cos(A) is an even function, the sign of A_H does not matter, and it can now be considered a triangle wave oscillating between 0 and 30°. Finally, frequency discrimination depends on effective frequency as $D(f)$, where $D(f)$ is the function shown in Fig. 4. The total function is then $D\{f_p \cos[A_H(A)]\}$. Note that both $A_H(A)$ and $D(f)$ are nonlinear functions, which will cause the hexagonal component to have a harmonic structure containing multiples of the basic 60° periodicity. Further, the exact shape of the function will depend quite critically on f_p since $D(f)$ is such a strongly nonlinear function in the region of the transition. This severe nonlinearity makes measurement of the exact shape of the transition difficult. If the exact shape were known, an exact prediction could be made for the hexagonal component, but lacking this we use the generalized component structure described in the text [Eq. (2)].
14. Locating the transition regions is fairly critical for this experiment. In an initial set of data we gathered $\Delta f/f$ versus orientation for observer SC at a reference frequency of 4.5 c/deg (the transition region for JH) and observed a much smaller effect. We subsequently gathered the data in Fig. 4 and found that the transition frequency for SC was approximately 0.5 c/deg lower than for JH. The hexagonal orientation effects were indeed much stronger for SC at a reference frequency of 4.0 [Fig. 1(a)].
15. G. Westheimer and S. McKee, "Spatial configurations for visual hyperacuity," Vision Res. **17,** 941–947 (1977).
16. The gap size of 0.25 deg for the vernier experiments was chosen in the expectation that the vernier threshold versus 1/gap size function would have a transition similar to that in Fig. 4 for this gap size, and preliminary measurements are consistent with this expectation.
17. D. O. Bowker, "Variations is apparent spatial frequency with stimulus orientation: II. Matching data collected under normal and interferometric viewing conditions," Percept. Psychophys. **29,** 568–577 (1981).
18. D. O. Bowker, "Variations in apparent spatial frequency with stimulus orientation: I. Incidence of the effect in the general population," Percept. Psychophys. **29,** 563–567 (1981).
19. M. A. Georgeson, "Spatial frequency analysis in early visual processing," Phil. Trans. R. Soc. Lond. B **290,** 11–22 (1980).
20. J. I. Yellott, Jr., "Spectral analysis of spatial sampling by photoreceptors: topological disorder prevents aliasing," Vision Res. **22,** 1205–1210 (1982).
21. J. Hirsch and R. Hylton, "Quality of the primate photoreceptor lattice and limits of spatial vision," Vision Res. (to be published).